

Laminar Flow in the Entrance Region of a Cylindrical Tube:

Part I. Newtonian Fluids

N.D. SYLVESTER and S. L. ROSEN

Carnegie-Mellon University, Pittsburgh, Pennsylvania

Pressure losses at the sharp edged entrance to a cylindrical tube were investigated for glycerine-water solutions over a Reynolds number range of 6 to 2,000.

For the experimental area contraction ratio of 0.0156, the Hagenbach (K) and Couette (K') coefficients are 2.4 and 295, respectively. Comparison with limited previous work shows that both coefficients increase with the area contraction ratio β over range $0 < \beta < 0.162$.

When a fluid enters a tube from a larger reservoir, the velocity distribution undergoes development until a fully developed equilibrium profile is reached some distance down the tube. Correspondingly, the pressure gradient in the region of flow development (the entrance length or hydrodynamic entrance region) differs from that in the region of fully developed flow. In view of the great technical importance of tube flows, there has been considerable interest in establishing the detailed nature of the flow in this region. However, even under laminar conditions, the equations of motion do not yield an exact solution, due largely to the presence of nonlinear inertial terms.

In this work, the excess entrance pressure drop ΔP_{ent} is defined as the difference between the observed pressure drop from a plane immediately upstream of the entrance to one in the region of fully developed flow and the pressure drop which would exist between the same planes if only losses from fully developed flow were present. The effective entrance length x_{eff} is the length of tube necessary to generate ΔP_{ent} under conditions of equilibrium flow in the downstream tube. These quantities are shown on a schematic pressure profile in Figure 1. Note that their specification requires that fully developed, equilibrium flow be reached in the tube and be maintained over a sufficient length to allow an accurate determination of the equilibrium pressure gradient.

A recent paper by Astarita and Greco (1) reviews much of the previous work for Newtonian fluids and presents the only published data for ΔP_{ent} for a sharp edged contraction $\beta = 0.1616$. A more extensive review of existing knowledge has been given recently by Holmes (7), who proposed the equation

$$g_c \frac{\Delta P_{\text{ent}}}{\frac{1}{2} \rho V^2} = K + K'/N_{Re} \quad (1)$$

which accommodates almost all of the previously published results. The terms K and K'/N_{Re} have often been referred to as the *Hagenbach* and *Couette corrections*, respectively. Equation (1) is not a direct solution to the equations of motion for laminar flow through a sharp edged contraction but is deduced from dimensional considerations. However, boundary-layer analyses (2 to 4, 8, 10, 11, 14) (presumably valid at high Reynolds numbers) give results of the form $g_c \Delta P_{\text{ent}} / \frac{1}{2} \rho V^2 = K$, and a creeping flow solution (15) (applicable at low N_{Re}) yields $g_c \Delta P_{\text{ent}} / \frac{1}{2} \rho V^2 =$

K'/N_{Re} which combined gives Equation (1). The published boundary-layer analyses generally assume no dissipation upstream of the entrance plane, a flat velocity profile at the entrance plane, and an infinite contraction ($\beta = 0$). These assumptions can be seriously violated for larger contraction ratios (1). LaNieve and Bogue (9) obtained a value for K' at very low N_{Re} and β which agrees well with that predicted by Weissberg's (15) creeping flow analysis.

EXPERIMENTAL

The flow loop consisted of a 55-gal. storage tank, pump, surge tank, and test section. The surge tank was a steel cylinder with dished, welded heads. A sight glass was provided to observe and maintain constant the liquid level within. Nitrogen pressure was used to adjust the level and to help fill the manometer lines. The entrance to the test section was made from a flanged 4 in. length of 4 in. I.D. steel pipe welded to the surge tank. The test section itself was an 8 ft. length of transparent acrylic tubing $\frac{1}{2}$ in. I.D., $\frac{3}{4}$ in. O.D., one end of which was glued through a $\frac{3}{4}$ in.

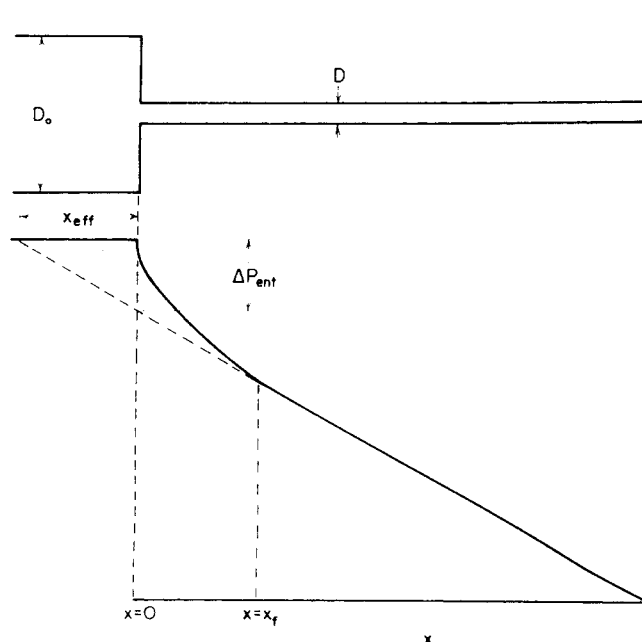


Fig. 1. Schematic pressure profile.

N. D. Sylvester is at Notre Dame University, Notre Dame, Indiana.

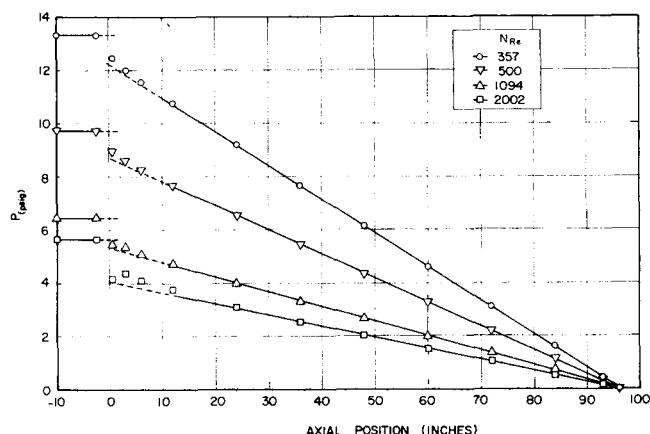


Fig. 2. Representative pressure profiles.

thick acrylic flange. The end of the tube was machined flush with the inside of the flange, so that when the steel and acrylic flanges were bolted together, a 180 deg. square edged entrance $D/D_0 = 1/8$ was formed. Pressure tap holes were 0.04-in. diameter and located alternately on opposite sides of the horizontal center line. The axial location of the pressure taps is recorded in Table 1.

Standard U tube manometers were connected between the pressure taps. A variety of manometric fluids from carbon tetrachloride to mercury was used to provide adequate readings. The lines and manometer tubes above the manometric fluid were completely filled with the test solution. The minimum precision of the pressure measurements was ± 0.01 lb./sq.in. (0.02 in. Hg).

The test fluids were circulated by a gear pump with a variable speed drive. The storage tank was equipped with a stirrer and an electric heater and on-off controller which maintained the test fluids at $30^\circ \pm 0.5^\circ\text{C}$. Flow rates were determined by weighing a timed portion of the tube effluent and densities determined with a hydrometer. Solution viscosities were checked with a standard Ubbelohde viscometer in a constant temperature bath maintained at $30^\circ \pm 0.02^\circ\text{C}$. The Newtonian test fluids were 30 to 96.5% solutions of glycerine in water. Further experimental details are available (12).

RESULTS AND DISCUSSION

Some representative pressure profiles are shown in Figure 2. The data at higher Reynolds numbers clearly indi-

TABLE 1

(0.0 = entrance plane)
(96.5 = exit plant)

Pressure tap number	Axial location, inches
1	-10
2	-2.5
3	0.5
4	3.0
5	6.0
6	12.0
7	24
8	36
9	48
10	60
11	72
12	84
13	93
14	96

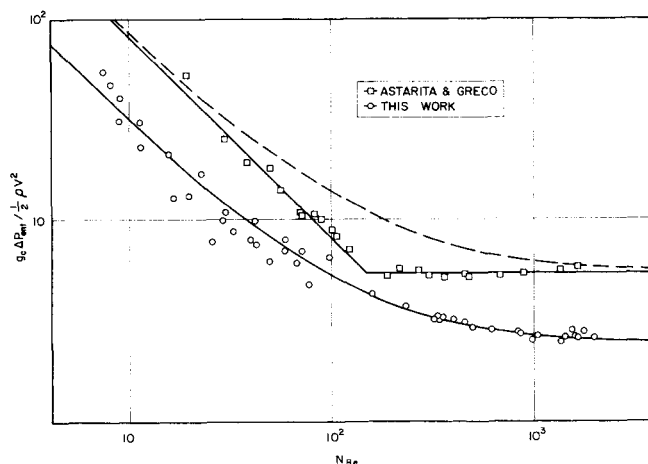


Fig. 3. Dimensionless entrance loss vs. Reynolds number

$$\begin{aligned} \text{---} \Delta P_{\text{ent}} / \frac{1}{2} \rho V^2 &= 5.48 + 795/N_{Re} \\ \text{—O—} \Delta P_{\text{ent}} / \frac{1}{2} \rho V^2 &= 2.4 + 295/N_{Re} \end{aligned}$$

cate the presence of a vena contracta, the intensity of which increased with N_{Re} as was observed by Astarita and Greco (1). This would be impossible if the velocity profile were flat at the entrance plane. Direct experimental evidence by Uebler (13) and the analysis of Wang and Longwell (14) have also shown that the velocity profile at the entrance plane is not flat.

The equilibrium pressure gradient ($\partial P / \partial x$) was statistically obtained from the pressure profiles. A least-squares line was fitted to the last three points. This line was projected back to the position of the next tap upstream and the projected pressure compared with the experimental value. If the experimental value was within two standard deviations of the predicted, the point was included in the least-squares line. This procedure was repeated until two successive points exceeded twice the standard deviation of the previously determined line. The last two points were then discarded, giving an objective value of ($\partial P / \partial x$). In all cases, viscosities calculated by using the gradient obtained were within 2% of those measured with the Ubbelohde viscometer.

The dimensionless entrance pressure drops $g_c \frac{\Delta P_{\text{ent}}}{\frac{1}{2} \rho V^2}$

are shown as a function of Reynolds number in Figure 3. The curve drawn is Equation (1) with $K = 2.4$ and $K' = 295$. The uncertainties in the coefficients are ± 0.1 and ± 50 , respectively. The equation represents the data quite well over the entire range of Reynolds numbers studied. This is to be contrasted with the results of Astarita and Greco (1); they concluded that for $\beta = 0.1616$

$$N_{Re} < 146; g_c \frac{\Delta P_{\text{ent}}}{\frac{1}{2} \rho V^2} = 795/N_{Re} \quad (2)$$

$$N_{Re} > 146; g_c \frac{\Delta P_{\text{ent}}}{\frac{1}{2} \rho V^2} = 5.48 \quad (3)$$

However, the summation of Equations (2) and (3), in the form of Equation (1), does not represent their data well at all, as also shown in Figure 3; they obtained a much sharper break. The reasons for this discrepancy are not clear at present.

Table 2 compares the results of this work with some other investigations. It is apparent that both K and K' increase with β for $0 < \beta < 0.1616$, and although more data are clearly needed, Table 2 and Equation (1) provide a

TABLE 2

Investigation	Reference	$\beta = D^2/D_0^2$	K	K'	N_{Re} range
Astarita and Greco (exp)	1	0.1616	5.48	795	10 to 2,000
This work (exp)	12	0.0156	2.4	295	6 to 2,000
LaNieve and Bogue (exp)	9	0.00718	—	36.8	$6.75 \times 10^{-4} - 6.75 \times 10^{-3}$
Weissberg (theory)	15	0	—	37.7-43.6	Low (creeping flow)
Collins and Schowalter (theory)	5	0	2.32	—	High (boundary-layer analysis)

reasonable basis for engineering design. Beyond this range, however, caution must be exercised, because it would seem that there must be maxima in the K and K' vs. β relations, since the coefficients should vanish as β goes to one.

Since $\left(\frac{\partial P}{\partial x}\right) = \frac{\Delta P_{ent}}{x_{eff}}$ (see Figure 1), it is easily shown with the aid of the Hagen-Poiseuille equation that the data may be represented by the equivalent relation

$$\frac{x_{eff}}{D} = A(\beta) + B(\beta) N_{Re} \quad (4)$$

where

$$A = \frac{K'}{64} \quad \text{and} \quad B = \frac{K}{64} \quad (5)$$

Figure 4 compares the data with Equation (4), with A and B calculated from Equation (5). Also shown is the line $x_{eff}/D = 0.05 N_{Re}$ which has been recommended by Dodge (6) for Newtonian fluids. The discrepancy at high Reynolds numbers is not surprising, since it is now obvious that all the coefficients depend on the contraction ratio.

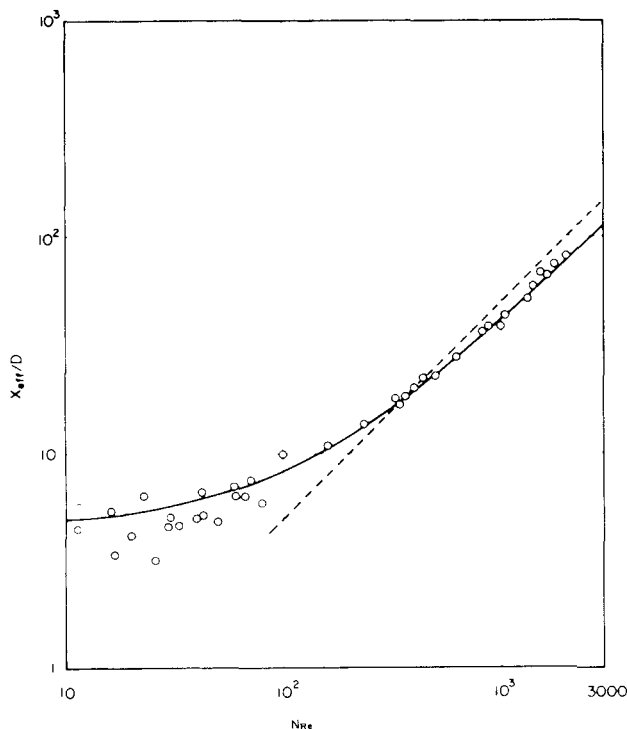


Fig. 4. Dimensionless effective entrance length vs. Reynolds number

$$-0 - \frac{x_{eff}}{D} = 4.61 + 0.0375 N_{Re}$$

$$- - \frac{x_{eff}}{D} = 0.05 N_{Re} \text{ [Dodge (6)]}$$

CONCLUDING REMARKS

Entrance effects for the laminar flow of Newtonian fluids through a sharp edged contraction are described well by Equations (1), (4), and (5). The exact nature of the variation of the coefficients with β requires further study.

ACKNOWLEDGMENT

The authors sincerely thank the National Science Foundation for support of this work.

NOTATION

- A, B = dimensionless coefficients defined in Equations (4) and (5)
 D = tube diameter, in.
 D_0 = reservoir diameter, in.
 g_c = conversion factor, in.-lb.m./lb.f. sec.²
 K = Hagenbach coefficient, dimensionless
 K' = Couette coefficient, dimensionless
 N_{Re} = Reynolds number
 P = pressure, lb./in.² (lb./sq.in.gauge)
 ΔP_{ent} = excess entrance pressure drop, lb./sq.in.gauge
 V = volumetric average velocity, ft./sec.
 x = axial distance, in.
 x_{eff} = effective entrance length, in.
 ρ = fluid density, lb.m./in.³
 $\beta = D^2/D_0^2$ = area contraction ratio

LITERATURE CITED

1. Astarita, G., and G. Greco, *Ind. Eng. Chem. Fundamentals*, **7**, 27 (1968).
2. Campbell, W. D., and J. C. Slaterry, *J. Basic Eng.*, **85**, 41 (1963).
3. Christiansen, E. B., and M. E. Lemmon, *AIChE J.*, **11**, 995 (1965).
4. Collins, M., and W. R. Schowalter, *Phys. Fluids*, **5**, 1122 (1962).
5. ———, *AIChE J.*, **9**, 804 (1963).
6. Dodge, D. W., Ph.D. thesis, Univ. Dela., Newark (1959).
7. Holmes, D. B., dissertation, Delft (1967).
8. Langhaar, H. L., *J. Appl. Mech.*, **9** A55 (1942).
9. LaNieve, H. L., and D. C. Bogue, *J. Appl. Poly. Sci.*, **12**, 353 (1968).
10. Schiller, L., *Z. Angew. Math. Mech.*, **2**, 96 (1922).
11. Sparrow, E. M., and S. H. Lin, *Phys. Fluids*, **7**, 338 (1964).
12. Sylvester, N. D., Ph.D. thesis, Carnegie-Mellon Univ., Pittsburgh, Pa. (1968).
13. Uebler, E. A., Ph.D. thesis, Univ. Dela., Newark (1966).
14. Wang, Y. L., and P. A. Longwell, *AIChE J.*, **10**, 323 (1964).
15. Weissberg, H. L., *Phys. Fluids*, **5**, 1033 (1962).

Manuscript received November 25, 1968; revision received February 26, 1969; paper accepted April 2, 1969.